

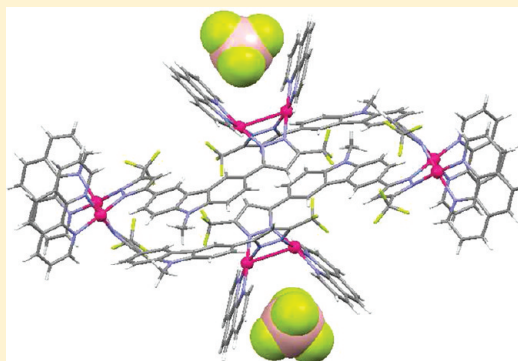
Self-Assembly of $[M_8L_4]$ and $[M_4L_2]$ Fluorescent Metallomacrocycles with Carbazole-Based Dipyrazole Ligands

Lin Qin, Liao-Yuan Yao, and Shu-Yan Yu*

Laboratory for Self-Assembly Chemistry, Department of Chemistry, Renmin University of China, Beijing 100872, People's Republic of China

Supporting Information

ABSTRACT: Fluorescent carbazole-based dipyrazole ligands (H_2L^{1-4}) were employed to coordinate with dipalladium corners ($[(phen)_2Pd_2(NO_3)_2](NO_3)_2$, $[(dmbpy)_2Pd_2(NO_3)_2](NO_3)_2$, or $[(15-crown-5-phen)_2Pd_2(NO_3)_2](NO_3)_2$, where phen = 1,10-phenanthroline and dmbpy = 4,4'-dimethyl-2,2'-bipyridine, in aqueous solution to afford a series of positively charged $[M_8L_4]^{8+}$ or $[M_4L_2]^{4+}$ multimetallomacrocycles with remarkable water solubility. Their structures were characterized by 1H NMR spectroscopy, electrospray ionization mass spectrometry, and elemental analysis and in the cases of $1 \cdot 8BF_4^-$ ($[(phen)_8Pd_8L_4](BF_4)_8$), and $3 \cdot 4BF_4^-$ ($[(phen)_4Pd_4L_2](BF_4)_4$) by single-crystal X-ray diffraction analysis. Complexes 3–8 are square-type hybrid metallomacrocycles, while complexes 1 and 2 exhibit folding cyclic structures. Interestingly, in single-crystal structures of $1 \cdot 8BF_4^-$ and $3 \cdot 4BF_4^-$, BF_4^- anions are trapped in the dipalladium clips through anion– π interaction. The luminescence properties and interaction toward anions of these metallomacrocycles were discussed.



INTRODUCTION

With the development of the field of self-assembly of supramolecular coordination complexes,¹ considerable research interest has been devoted to constructing well-defined coordination or organometallic supramolecular architectures with novel structures^{2–4} and promising applications in guest inclusion,⁵ catalysis,⁶ luminescence,^{7,8} and anion complexation.⁹

Owing to the important roles that anions play in chemistry, biology, and environment, great efforts have been made in the design and synthesis of receptors for anions, most of which are capable of interacting with anions through hydrogen bonds in organic systems and other intramolecular and intermolecular interactions.⁹ To the best of our knowledge, although chemists have showed increasing interest in sensing anions based on metal–organic compounds,¹⁰ self-assembled metallomacrocycles utilized to interact with anion selectivity in aqueous solution are rare. Recently, we developed a metal-directed self-assembly approach to constructing supramolecular metallomacrocycles with good water solubility,^{11,12} some of which show potential application in the complexation of anions.¹¹

Herein, by employing functional dipyrazoles^{13,14} with fluorescent carbazole groups to self-assemble with different dipalladium clips, we synthesized a series of square-type hybrid $[M_4L_2]^{4+}$ and folding $[M_4L_2]^{4+}$ metallomacrocycles, especially obtaining an unprecedented $[M_8L_4]^{8+}$ metallomacrocyclic structure in aqueous solution. The properties for luminescent metallomacrocycles in anion interaction were studied through UV–vis, fluorescent, and NMR experiments,

indicating that the folding $[M_8L_4]^{8+}$ structure presented interaction with an SCN^- anion.

RESULT AND DISCUSSION

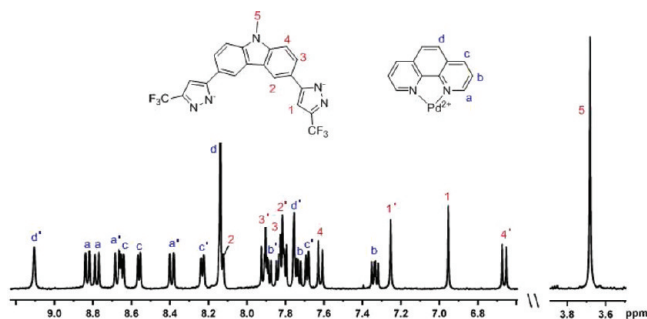
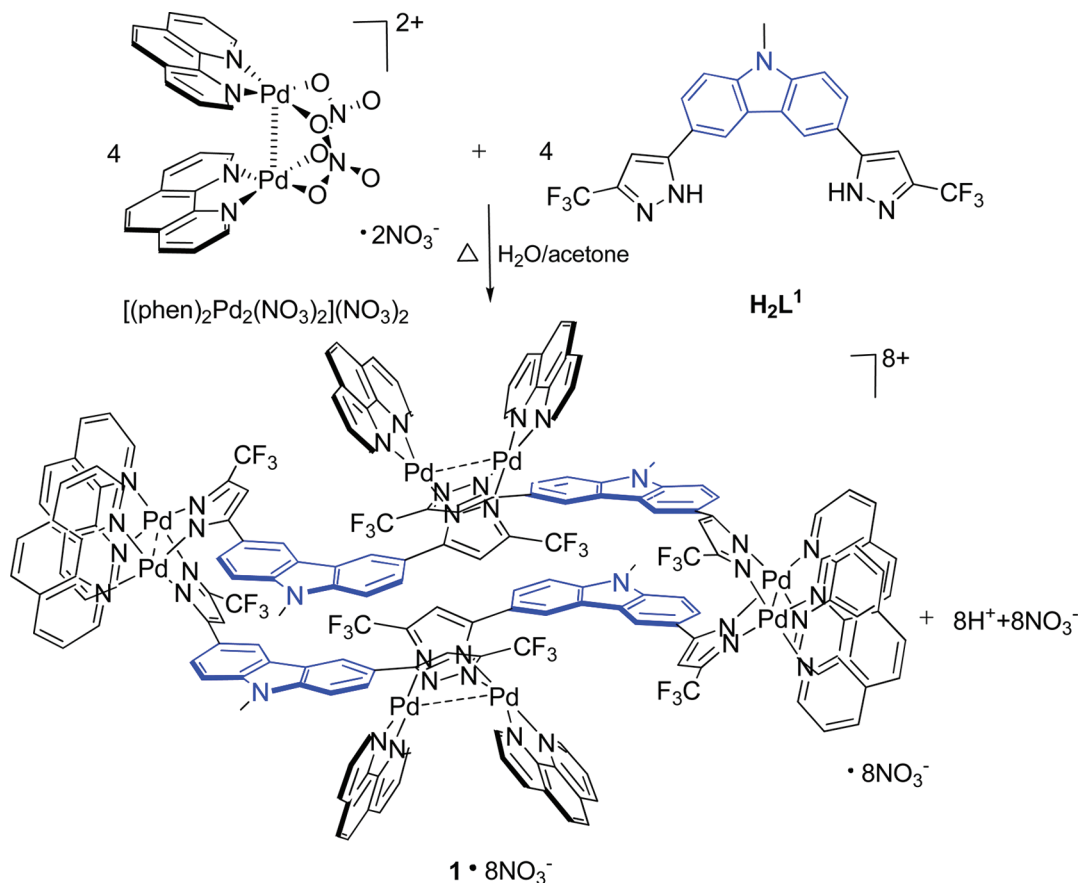
Self-assembly and Characterization of the $[M_8L_4]^{8+}$ Metallomacrocyclic. As shown in Scheme 1, $[(phen)_2Pd_2(NO_3)_2](NO_3)_2$ was treated with a suspension containing 1 equiv of H_2L^1 in H_2O (1 mL) and acetone (0.5 mL) at room temperature. After stirring for 2 h, the mixture was heated at 60 °C for another 24 h. The resulting yellow solution was then filtered and the clear filtrate was concentrated, leading to the formation of the positively charged folding metallomacrocyclic $1 \cdot 8NO_3^-$. The BF_4^- and PF_6^- salts were prepared by anion exchange with an excess of KBF_4 and KPF_6 , respectively.

The 1H NMR spectrum of $1 \cdot 8PF_6^-$ (the PF_6^- salt of **1**) is shown in Figure 1; it reveals proton resonances of the pyrazole groups of the ligand (L^1) at 7.25 and 6.95 ppm, which is different from the free dipyrazole ligand H_2L^1 , which shows only one singlet at 7.18 ppm. Furthermore, the signals of most original homotopic protons split into several peaks, except protons of methyl (methyl H_5) of the ligand, which indicates that these protons are in distinct chemical environments from each other in metallomacrocycles. The above phenomenon indicates a low-symmetrical folding architecture, with most

Received: November 8, 2011

Published: February 2, 2012

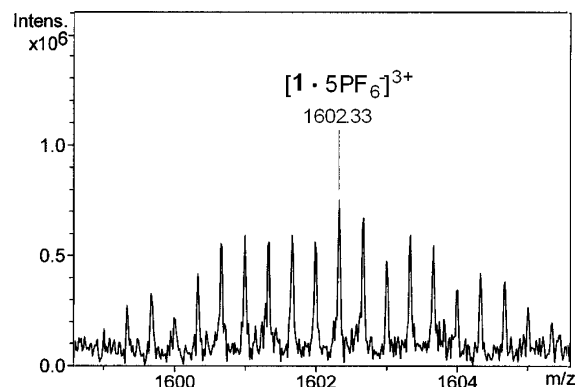


Scheme 1. Self-Assembly of the Folding $[M_8L_4]^{8+}$ MetallomacrocyclicFigure 1. 1H NMR spectrum of $1 \cdot 8PF_6^-$ in CD_3CN , $25^\circ C$, $Si(CH_3)_4$.

protons rigidly located, as further confirmed by X-ray structure analysis (see below).

The formation of the $[M_8L_4]^{8+}$ metallomacrocyclic was further demonstrated by an electrospray ionization mass spectrometry (ESI-MS) study, where multiply charged molecular ions corresponding to intact macrocycles were observed. The multiply charged ion of **1** was observed at m/z 1602.33, which is assigned to $[1 \cdot 5PF_6]^{3+}$ (Figure 2).

Finally, the formation of the $[M_8L_4]^{8+}$ metallomacrocyclic was confirmed by the single-crystal X-ray structure study of $1 \cdot 8BF_4^-$. Single crystals of $1 \cdot 8BF_4^-$ were obtained by the vapor diffusion of diethyl ether into its acetonitrile solution. Complex $1 \cdot 8BF_4^-$ crystallizes in the triclinic space group $P\bar{1}$. As shown in Figure 3, the crystal structure analysis reveals the folding metallomacrocyclic structure with four carbazole-based dipyrazole ligands bridged with four $[(phen)Pd^{II}]_2$ clips. The large dihedral angles (63.4° and 60.5°) of the $(phen)Pd^{II}$ planes

Figure 2. ESI-MS spectrum of $1 \cdot 8PF_6^-$ in CH_3CN : isotopic distribution of the species $[1 \cdot 5PF_6]^{3+}$.

within each corner indicate that there is no π - π -stacking interaction between them. This conformation also creates an "open clip" disposition for the square-planar environment of the two Pd atoms. The $Pd1 \cdots Pd2$ and $Pd3 \cdots Pd4$ separations at 3.087 and 3.178 Å are in the range of typical $Pd \cdots Pd$ interactions (2.60–3.30 Å).¹⁵ In the dipalladium corners, the dihedral angles between pyrazole planes N9–N10 and N14–N15 and between N12–N13 and N17–N18 are 77.8° and 62.5° , respectively. All of the bond lengths of $Pd-N$ are around 2.00 Å (Table S1 in the Supporting Information). Within one molecule, two carbazole planes are on one side, while the other two are on the opposite side, and the distance between the N16–C73–C74 and N11–C55–C56 planes is short (3.574 Å), resulting in a long-and-narrow cavity. Interestingly, the

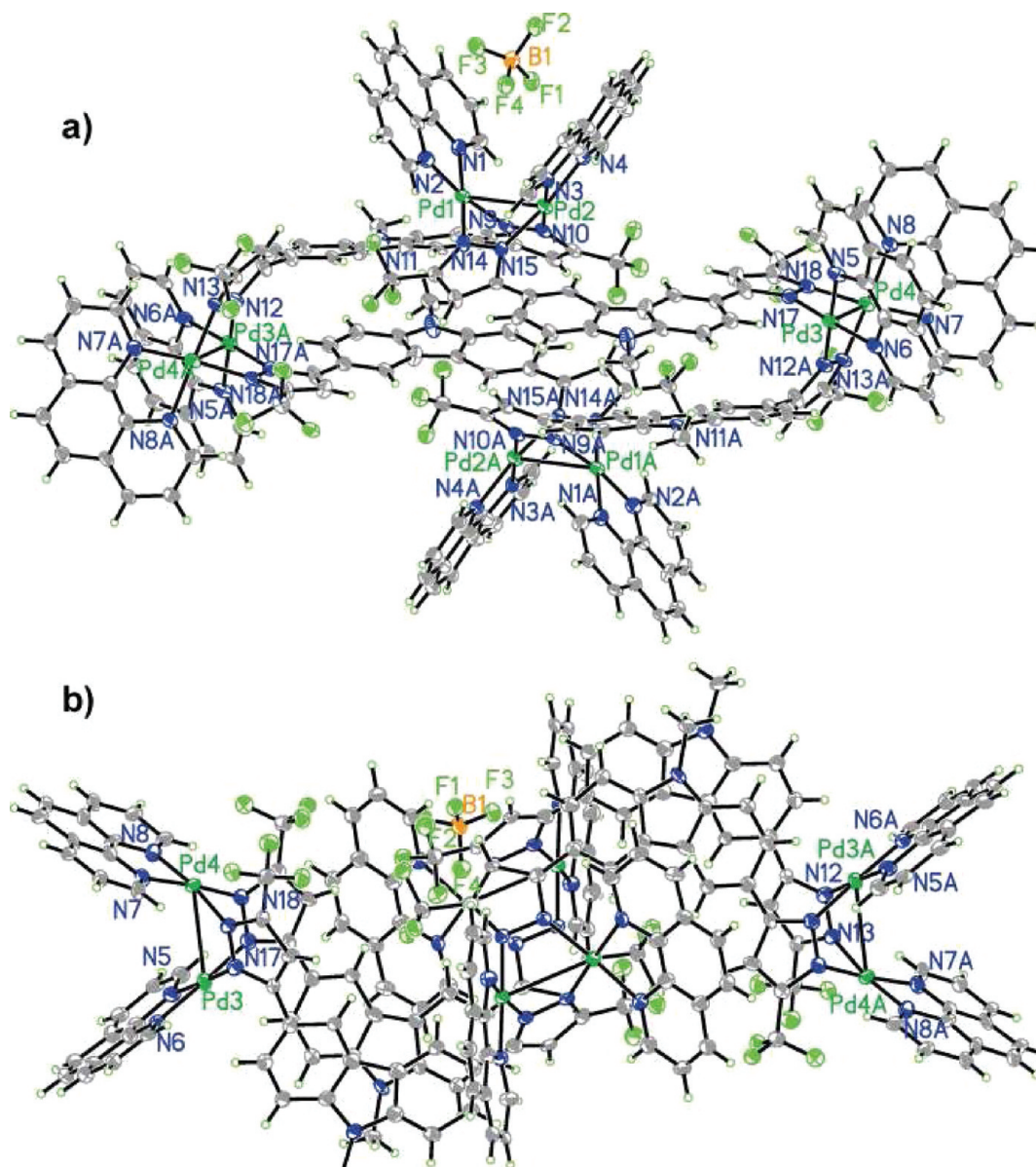


Figure 3. ORTEP diagrams of the molecular structure of $1 \cdot 8\text{BF}_4^-$: (a) top view; (b) side view. Thermal ellipsoids are shown at the 30% probability level. The remaining counteranions are omitted for clarity.

structure of $1 \cdot 8\text{BF}_4^-$ traps two BF_4^- anions through anion- π interaction into the clasp-like cavity formed by the (phen)Pd1 and (phen)Pd2 planes with contact distances of $\text{F1} \cdots \pi = 2.906$ Å and $\text{F2} \cdots \pi = 2.791$ Å. This distance is significantly shorter than the separations of this BF_4^- and palladium centers ($\text{Pd1} \cdots \text{Pd2}$ and $\text{Pd3} \cdots \text{Pd4}$), which indicates that the interaction of BF_4^- and the phen rings has a major effect in the trapping of BF_4^- . This result may be attributed to coordinated Pd^{II} atoms, which withdraw electron density from the phen rings and increase the affinity of the phen rings for the BF_4^- anion.^{16,17} Another BF_4^- is located at the side of the complex with $\text{C}-\text{H} \cdots \text{F}$ hydrogen-bonding interactions. As shown in the packing diagram (Figure 4), molecules of complex $1 \cdot 8\text{BF}_4^-$ pack through weak intermolecular $\pi-\pi$ -stacking interactions between the phen rings of neighboring molecules with a approximate contact distance of 3.881 Å. Anions are included in the crystal lattice by $\text{C}-\text{F} \cdots \pi$ interactions between $\text{C}-\text{F}$ and the aromatic rings and by $\text{C}-\text{H} \cdots \text{F}$ hydrogen bonds between

BF_4^- and the aromatic protons (Table S2 in the Supporting Information).

Self-Assembly and Characterization of the Folding $[\text{M}_4\text{L}_2]^{4+}$ Metallomacrocyclic. When ligand H_2L^1 was treated with $[(\text{dmbpy})_2\text{Pd}_2(\text{NO}_3)_2](\text{NO}_3)_2$ in the same ratio as **1** in a H_2O and acetone solution, a low-symmetrical ^1H NMR spectrum was presented (see Figure S8 in the Supporting Information). However, we obtained $[\text{M}_4\text{L}_2]^{4+}$ instead of $[\text{M}_8\text{L}_4]^{8+}$ metallomacrocyclic, which was supported by ESI-MS studies, as shown in Figure S18 in the Supporting Information. The multiply charged molecular ions of $2 \cdot 4\text{BF}_4^-$ at m/z 1115.61 and 713.74 are ascribed to $[2 \cdot 2\text{BF}_4^-]^{2+}$ and $[2 \cdot \text{BF}_4^-]^{3+}$, respectively. Compared to the rigid (phen)Pd^{II} clip, the (dmbpy)Pd^{II} clip is more flexible to adjusting its configuration in solution, leading to the formation of $2 \cdot 4\text{BF}_4^-$ with a small cavity of the $[\text{M}_4\text{L}_2]^{4+}$ structure. On the basis of the above studies and the crystal structure of **1**, this folding configuration was optimized with the CAChe6.1.1 program (Scheme 2).

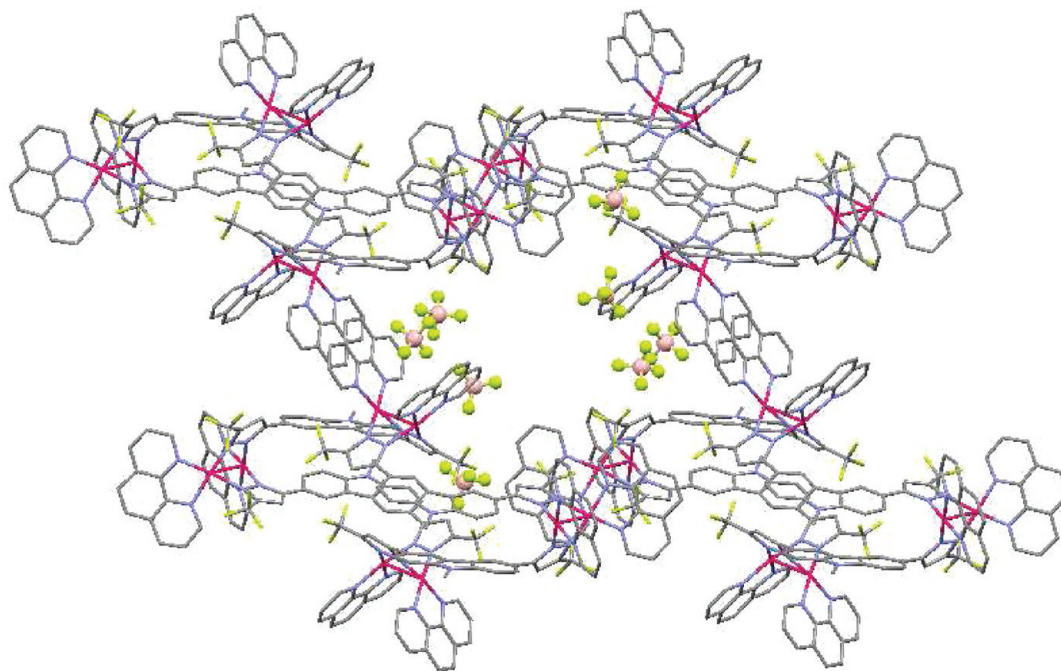


Figure 4. Packing diagram of 1·8BF₄[−].

Self-Assembly and Characterization of the Square-Type [M₄L₂]⁴⁺ Metallomacrocycles. As shown in Scheme 3, the fluorescent dipyrazole-bridged metallomacrocycles 3·4NO₃[−]–8·4NO₃[−] are self-assembled in aqueous solution. [(dmbpy)₂Pd₂(NO₃)₂](NO₃)₂, [(phen)₂Pd₂(NO₃)₂](NO₃)₂, or [(15-crown-5-phen)₂Pd₂(NO₃)₂](NO₃)₂ were treated with a suspension containing 1 equiv of H₂L², H₂L³, or H₂L⁴ (Scheme 4) in H₂O (1 mL) and acetone (0.5 mL) at room temperature. After stirring for 2 h, the mixture was heated at 60 °C for another 24 h. The resulting light-yellow solution was then filtered, and the clear filtrate was concentrated, leading to the formation of positively charged [M₄L₂]⁴⁺ [M = (phen)Pd^{II}, 3; M = (dmbpy)Pd^{II}, 4], [M₄L₃]⁴⁺ [M = (phen)Pd^{II}, 5; M = (dmbpy)Pd^{II}, 6], or [M₄L₄]⁴⁺ [M = (15-crown-5-phen)Pd^{II}, 7; M = (dmbpy)Pd^{II}, 8] metallomacrocycles with spontaneous deprotonation of the dipyrazole ligands. Their BF₄[−] or PF₆[−] salts were prepared by anion exchange with an excess of KBF₄ or KPF₆.

As shown in the ¹H NMR spectrum of 5·4BF₄[−] (Figure 5), signals exhibited at 8.85–8.87, 8.64–8.65, 8.20, and 8.02–7.99 ppm correspond to a, c, d, and b protons of the phen, respectively. Other signals belong to ligand L³. The corresponding resonances of the methylene and methyl groups of the ligand L³ appear in the upfield region, which reveals one singlet each at 5.73 and 2.68 ppm, respectively. ¹H NMR analyses of this product indicate the formation of a single species, and integration of the signals is indicative of a 2:1 ratio of the metal complex (phen)Pd^{II} fragment to the dipyrazole ligand.

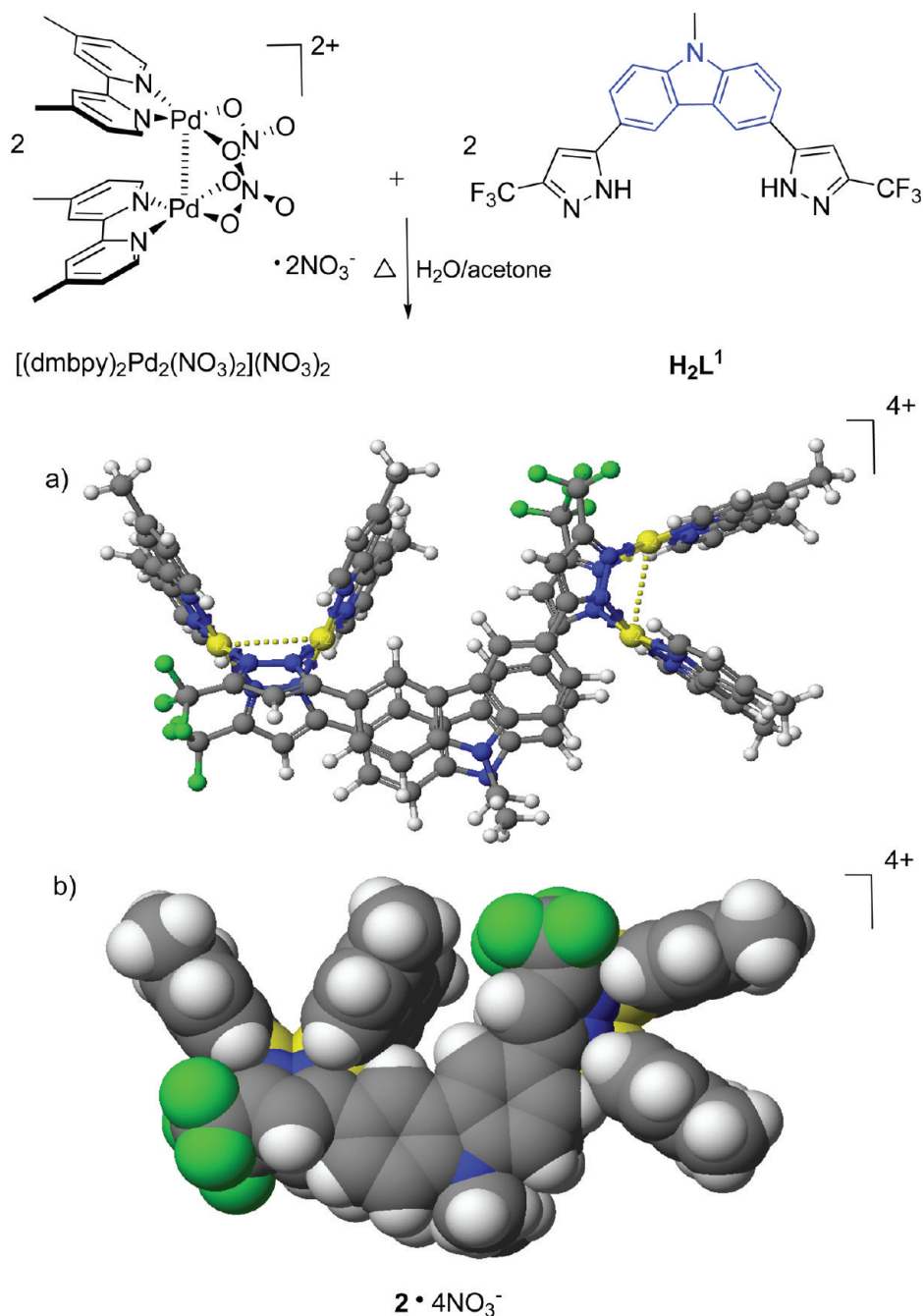
The formation of [M₄L₂]⁴⁺ metallomacrocyclic structures was further supported by ESI-MS measurement, allowing assignment of the [(phen)Pd]₄L₂²⁺, [(dmbpy)Pd]₄L₂²⁺, [(phen)Pd]₄L₃³⁺, [(dmbpy)Pd]₄L₃³⁺, [(15-crown-5-phen)Pd]₄L₂²⁺, and [(dmbpy)Pd]₄L₂²⁺ compositions, respectively. As shown in Figure 6, the multiply charged molecular ions of 5·4BF₄[−] were observed at *m/z* 1103.67 ([5·2BF₄[−]]²⁺), 706.44 ([5·BF₄[−]]³⁺), and 508.33 ([5]⁴⁺). Similarly, the multiply charged molecular

ions of 4·4BF₄[−] observed at *m/z* 661.45 and 474.39 (Figure S20 in the Supporting Information) corresponded to the cations [4·BF₄[−]]³⁺ and [4]⁴⁺, and the multiply charged molecular ions of 7·4PF₆[−] observed at *m/z* 1080.91 and 774.69 (Figure S22 in the Supporting Information) are assignable to cations [7·PF₆[−]]³⁺ and [7]⁴⁺, respectively.

By the vapor diffusion of diethyl ether into its acetonitrile solution, complex 3·4BF₄[−] crystallizes in the orthorhombic space group *Pbcn*. The complex displays a square-shape hybrid metallomacrocyclic structure with two pyrazole ligands doubly bridged by [(phen)Pd^{II}]₂ corners (Figure 7). Within each corner, an “open clip” disposition is exhibited with a large dihedral angle (70.3°) between the two (phen)Pd^{II} planes. The Pd1⋯Pd2 separation of 3.188 Å indicates typical Pd⋯Pd interactions (2.60–3.30 Å).¹⁵ The dihedral angle between the two pyrazole (N5–N6 and N8–N9) planes at the corner is 84.8°, which is smaller than the angles of N1–Pd1–N5 (94.0°), N2–Pd1–N8A (94.7°), N3–Pd2–N6 (94.2°), and N4–Pd2–N9A (91.4°). The most interesting feature of the structure is the binding of two BF₄[−] into the cliplike cavity formed by the (phen)Pd1 and (phen)Pd2 planes with contact distances of F1⋯π = 3.226 Å and F2⋯π = 3.168 Å. The anion–π interactions of BF₄[−] and the phen rings have a major effect on the binding of BF₄[−]. Another BF₄[−] is located at the side of the complex also by anion–π interaction. In the crystal, molecules of complex 3·4BF₄[−] pack by weak intermolecular π–π-stacking interactions involving phen and carbazole rings between neighboring molecules with an approximate contact distance of 3.50 Å.

Luminescent Properties and Interaction toward Anions. As shown in Figure 8, in dimethyl sulfoxide (DMSO)/H₂O (3:1, v/v), H₂L¹ exhibits characteristic carbazole emission and fluorescence maxima at 378 and 398 nm and UV–vis spectral peaks at 258 and 298 nm, respectively. When [(phen)₂Pd₂(NO₃)₂](NO₃)₂ was added in H₂L¹, the emission intensity of H₂L¹ in fluorescent spectra was quenched sharply because of coordination between N atoms of pyrazole

Scheme 2. Self-Assembly and Optimized Configuration of $[M_4L_2]^{4+}$ Metallomacrocyclic- $2 \cdot 4NO_3^-$ Optimized with the CAChe6.1.1 Program (See Ref 18)^a

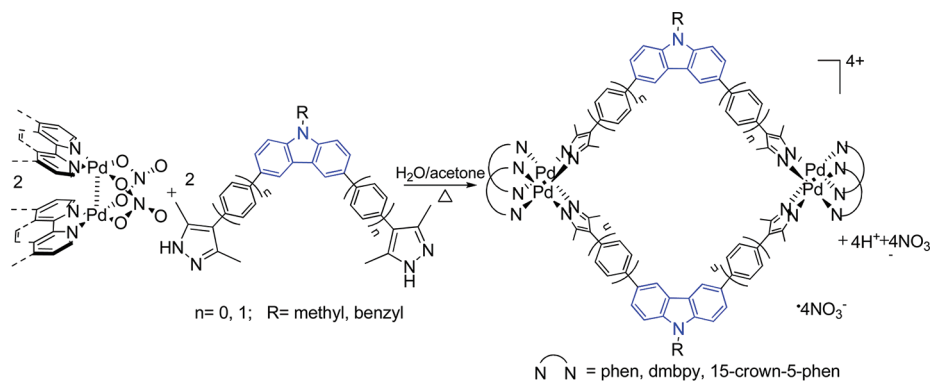


^a(a) Ball-and-stick model and (b) space-and-stack model. (yellow, Pd; gray, C; white, H; green, F; blue, N).

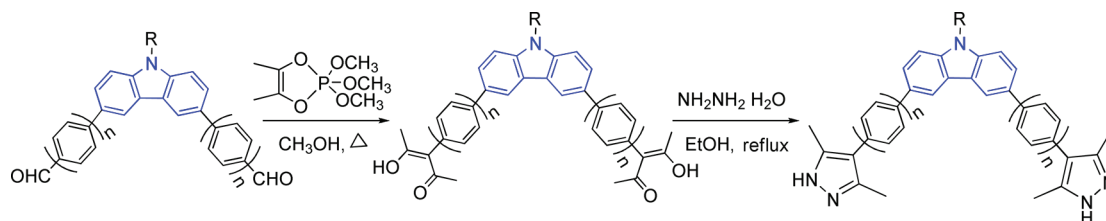
and Pd atoms and distortion effects on the emission quantum yield (Φ_{em}) of the carbazole rings, while the absorption intensity of L^1 in UV-vis spectra increased notably. A similar phenomenon was also observed in the emission and absorbance of H_2L^2 , H_2L^3 , and H_2L^4 ligands (Figures S24–S26 in the Supporting Information).

The effects of anions (K^+ salts) on the fluorescent emission intensity of metallomacrocyclics $1 \cdot 8PF_6^-$, $4 \cdot 4BF_4^-$, $5 \cdot 4BF_4^-$, and $8 \cdot 4PF_6^-$ (1.5×10^{-6} M) were investigated in a DMSO/ H_2O (3:1, v/v) solution at room temperature. Upon the addition of 1000 equiv of BF_4^- , Br^- , Cl^- , F^- , $H_2PO_4^-$, Γ^- , N_3^- , NO_3^- , and SO_4^{2-} anions, no remarkable fluorescence intensity changes

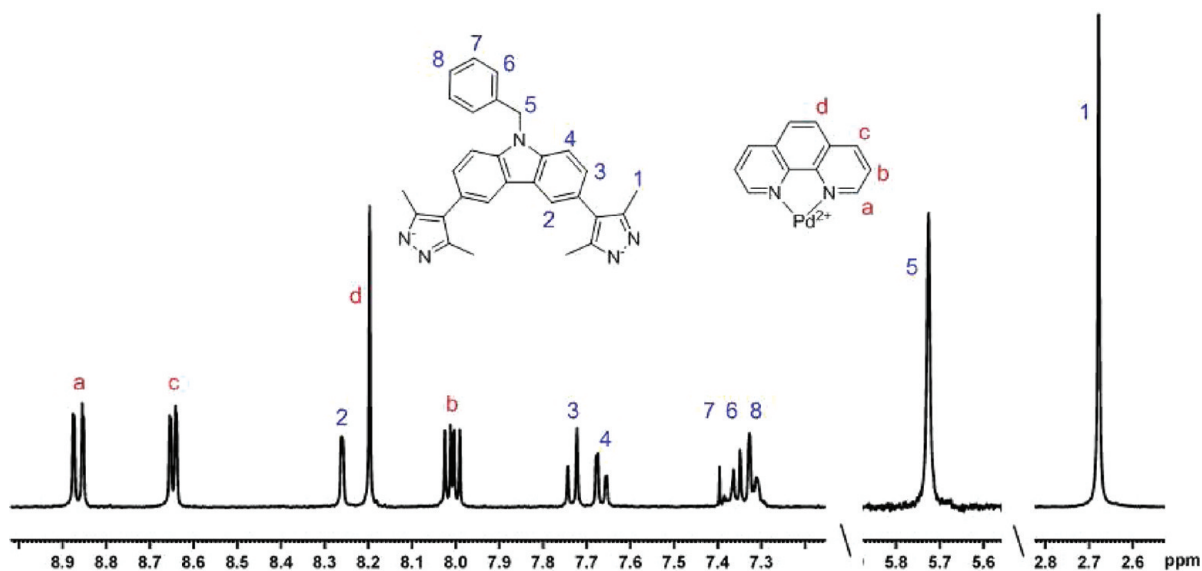
were observed. However, we noticed fluorescence enhancement upon the addition of SCN^- (1000 equiv) to $1 \cdot 8PF_6^-$ (Figure 9), while no change was observed upon application to three other metallomacrocyclics (Figures S27–S29 in the Supporting Information). Fluorescence titration experiments were carried out as well; nevertheless, no intensity enhancement was observed until the addition of 100 equiv of SCN^- , as shown in Figure S31 in the Supporting Information. 1H NMR experiments of the $1 \cdot 8PF_6^-$ complex were carried out before and after the addition of 1000 equiv of SCN^- in a DMSO- d_6 / D_2O (3:1, v/v) solution (Figure S32 in the Supporting Information); we noticed that the number of peaks decreased

Scheme 3. Self-Assembly of Square-Type Hybrid $[M_4L_2]^{4+}$ Metallomacrocycles

| | | |
|---|------------------------|--------------------------|
| $[(\text{phen})_2\text{Pd}_2(\text{NO}_3)_2](\text{NO}_3)_2$ | H_2L^2 | $3 \cdot 4\text{NO}_3^-$ |
| $[(\text{dmbpy})_2\text{Pd}_2(\text{NO}_3)_2](\text{NO}_3)_2$ | H_2L^2 | $4 \cdot 4\text{NO}_3^-$ |
| $[(\text{phen})_2\text{Pd}_2(\text{NO}_3)_2](\text{NO}_3)_2$ | H_2L^3 | $5 \cdot 4\text{NO}_3^-$ |
| $[(\text{dmbpy})_2\text{Pd}_2(\text{NO}_3)_2](\text{NO}_3)_2$ | H_2L^3 | $6 \cdot 4\text{NO}_3^-$ |
| $[(15\text{-crown-5-phen})_2\text{Pd}_2(\text{NO}_3)_2](\text{NO}_3)_2$ | H_2L^4 | $7 \cdot 4\text{NO}_3^-$ |
| $[(\text{dmbpy})_2\text{Pd}_2(\text{NO}_3)_2](\text{NO}_3)_2$ | H_2L^4 | $8 \cdot 4\text{NO}_3^-$ |

Scheme 4. Synthesis of Fluorescent Dipyrzole Ligands H_2L^2 , H_2L^3 , and H_2L^4 

| | | | |
|------------|-------|----------|------------------------|
| R = Methyl | n = 0 | a | H_2L^2 |
| benzyl | 0 | b | H_2L^3 |
| benzyl | 1 | c | H_2L^4 |

Figure 5. ^1H NMR spectrum of $5 \cdot 4\text{BF}_4^-$ in CD_3CN , 25°C , $\text{Si}(\text{CH}_3)_4$ (1–8, blue, signals of L^3 ; a–d, red, signals of phen).

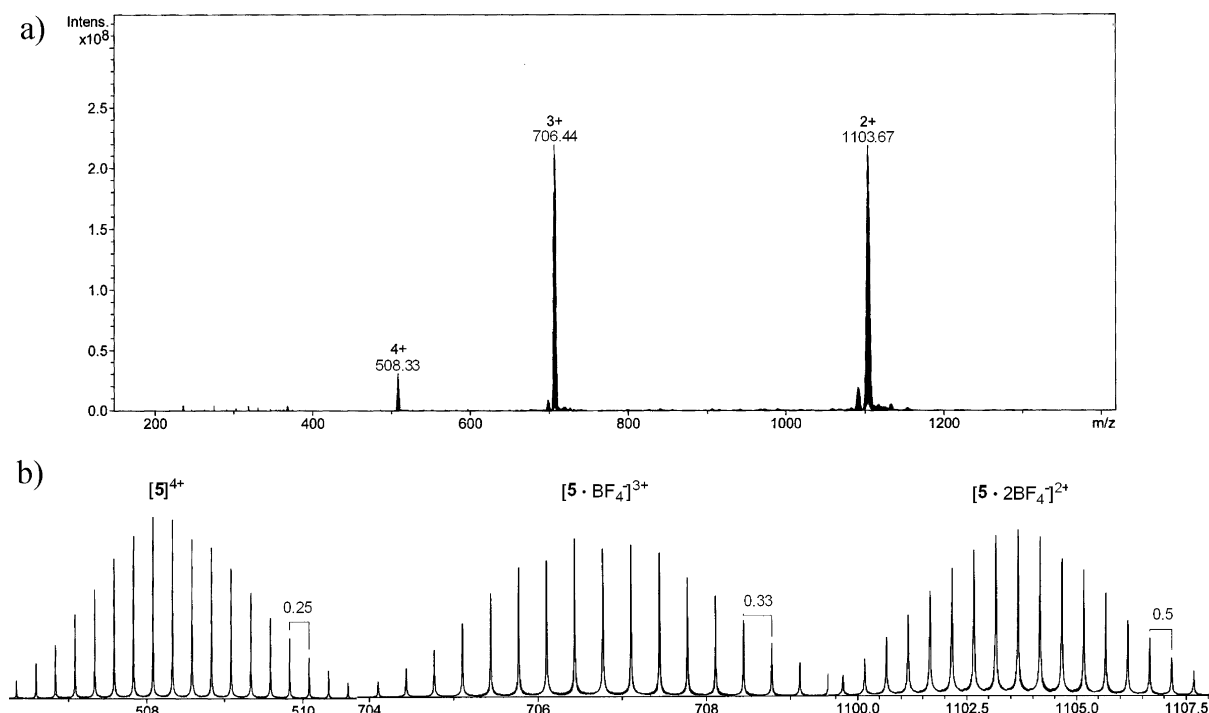


Figure 6. (a) ESI-MS spectrum of $5 \cdot 4\text{BF}_4^-$ in acetonitrile. (b) Isotopic distribution of the species $[5 \cdot 2\text{BF}_4^-]^{2+}$, $[5 \cdot \text{BF}_4^-]^{3+}$, and $[5]^{4+}$.

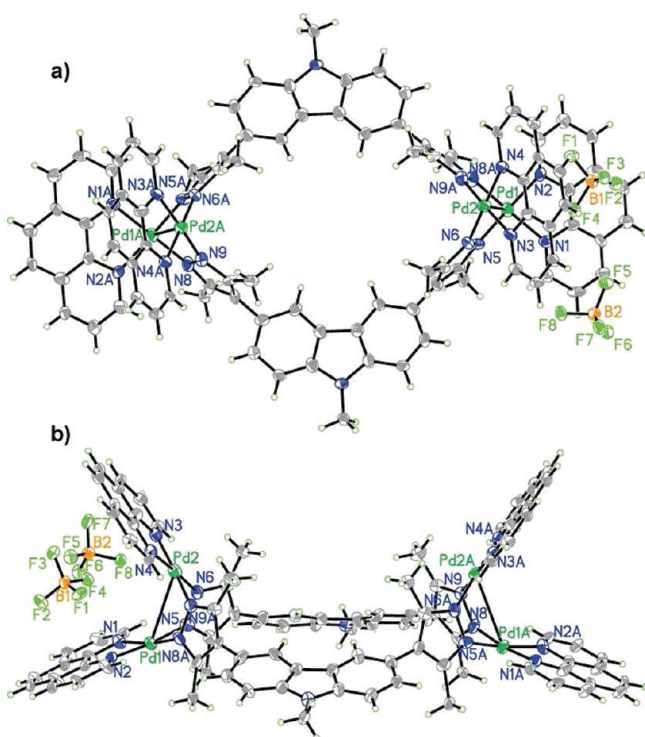


Figure 7. ORTEP diagrams of the molecular structure of $3 \cdot 4\text{BF}_4^-$: (a) top view; (b) side view. Thermal ellipsoids are shown at the 30% probability level.

and the ratio of the L^1 ligand and phen ring of dipalladium clips turned to 1:1 from 1:2. On the basis of the above research, we proposed that, because of the competitive coordination ability of SCN^- and carbazole-based dipyrzole as well as the higher tension of the $1 \cdot 8\text{PF}_6^-$ folding structure, the coordination site of the $1 \cdot 8\text{PF}_6^-$ metallomacrocyclic was more likely to be weakened by SCN^- , finally leading to partial decomposition of

dipalladium clips. As a result, quenching caused by metal–organic complexes was inhibited, resulting in the revival of fluorescence.

CONCLUSIONS

A series of metallomacrocycles with good water solubility can be obtained in nearly quantitative yield based on fluorescent carbazole–dipyrzole ligands and dipalladium clips via a directed self-assembly process. The assemblies have been characterized by elemental analysis, ^1H NMR, and ESI-MS and in the cases of **1** and **3** by a single-crystal X-ray diffraction method. These characterizations show that novel $[\text{M}_8\text{L}_4]^{8+}$ and $[\text{M}_4\text{L}_2]^{4+}$ metallomacrocycles with different size and shape can be obtained by fine-tuning of the carbazole ligands and dipalladium corners. The single-crystal structures present that the dipalladium clips of these metallomacrocycles can interact with BF_4^- anions. In addition, the UV–vis absorption and fluorescence emission intensity of ligands and metallomacrocycles and interaction toward anions have been investigated as well, which show that complex $1 \cdot 8\text{PF}_6^-$ selectively interacts with SCN^- anions in aqueous solution.

EXPERIMENTAL SECTION

Materials. Potassium hexafluorophosphate (99%) and sodium tetrafluoroborate (99%) were purchased from Acros Organics and used without further purification. All other chemicals and solvents were of reagent grade and were purified according to conventional methods.¹⁹ The dimetal clips $[(\text{dmbpy})_2\text{Pd}_2(\text{NO}_3)_2](\text{NO}_3)_2$,^{15,16} $[(\text{phen})_2\text{Pd}_2(\text{NO}_3)_2](\text{NO}_3)_2$,²⁰ and $[(15\text{-crown-5-phen})_2\text{Pd}_2(\text{NO}_3)_2](\text{NO}_3)_2$ ²¹ (where dmbpy = 4,4'-dimethyl-2,2'-bipyridine and phen = 1,10-phenanthroline) were prepared according to literature procedures. Compounds 9-methylcarbazole-3,6-dicarbaldehyde,²² 9-benzylcarbazole-3,6-dicarbaldehyde,²² 4,4'-(9-benzylcarbazole-3,6-diyl)-dibenzaldehyde,²³ and 1,1'-(9-methylcarbazole-3,6-diyl)bis(4,4,4-trifluorobutane-1,3-dione)²⁴ were synthesized according to published methods.

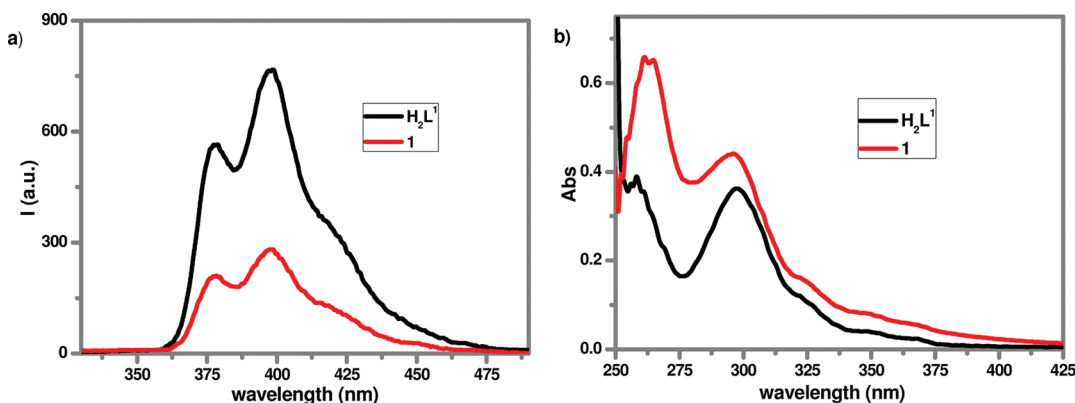


Figure 8. (a) Fluorescence emission spectra and (b) UV-vis absorption spectra of H_2L^1 and $1 \cdot 8PF_6^-$ in DMSO/ H_2O (3:1, v/v). $\lambda_{ex} = 300$ nm.

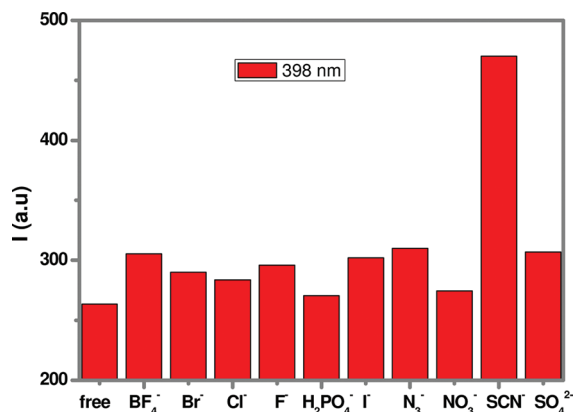


Figure 9. Fluorescent intensity of $1 \cdot 8PF_6^-$ at 398 nm upon the addition of excessive BF_4^- , Br^- , Cl^- , F^- , $H_2PO_4^-$, I^- , N_3^- , NO_3^- , SCN^- , and SO_4^{2-} anions in DMSO/ H_2O (3:1, v/v; 1.5×10^{-6} M). $\lambda_{ex} = 300$ nm.

Instrumentation. 1H and ^{13}C NMR experiments were performed on a Bruker Avance DMX400 spectrometer using tetramethylsilane [$Si(CH_3)_4$] as an internal standard. A visual molecular model was computed using the CAChe6.1.1 program¹⁸ to evaluate the shape of macrocycle **2**. ESI-MS measurements were performed with an HP5989B mass spectrometer. Elemental analysis was performed on a Thermoquest Flash EA 1112 instrument. UV-visible absorption spectra were obtained on a Cary 50 Probe UV-visible spectrophotometer. Fluorescence spectra were measured using a PerkinElmer Instruments luminescence spectrophotometer. Fluorescent titrations were carried out by adding aliquots of various anions as their K^+ salts to $1 \cdot 8PF_6^-$ (1.5×10^{-6} M) in DMSO/ H_2O (3:1, v/v) at 25 °C. Excitation was at 300 nm. Both excitation and emission slit widths were 3 nm.

X-ray Structural Determinations. All single-crystal X-ray diffraction data were collected on a Bruker Smart Apex CCD area detector equipped with graphite-monochromated Mo $K\alpha$ radiation ($\lambda = 0.71073$ Å). Multiscan absorption correction for all complexes was performed using the SADABS program.²⁵ All structures were solved by direct methods, refined employing full-matrix least squares on F^2 by using the SHELXTL (Bruker, 2000) program, and expanded using Fourier techniques.²⁶ The locations of the Pd atoms were determined, and all non-H atoms of these complexes were refined anisotropically. H atoms were included in idealized positions and refined with fixed geometry with respect to their carrier atoms. Refinement data were processed by using the SQUEEZE program. All of the crystal data and structure refinement details, such as the unit cell, space group, data collection, and refinement parameters, are presented in Table 1.

Synthesis. *Synthesis of Organic Ligands. General Procedure for Acetylacetone.*²⁷ A 5 mL CH_2Cl_2 solution of dialdehyde (8.4 mmol), biacetyl, and trimethyl phosphite adduct (11 mL) was stirred

Table 1. Crystallographic Data for Complexes $1 \cdot 8BF_4^-$ and $3 \cdot 4BF_4^-$

| | $1 \cdot 8BF_4^-$ | $3 \cdot 4BF_4^-$ |
|---|-------------------------------------|-----------------------------------|
| formula | $C_{180}H_{108}F_{36}N_{36}B_8Pd_8$ | $C_{94}H_{74}N_{18}B_4F_{16}Pd_4$ |
| fw | 4776.70 | 2228.55 |
| cryst syst | triclinic | orthorhombic |
| space group | $P\bar{1}$ | $Pbcn$ |
| temp (K) | 153(2) | 291(2) |
| <i>a</i> [Å] | 18.2309(2) | 21.622(2) |
| <i>b</i> [Å] | 18.4937(1) | 30.812(3) |
| <i>c</i> [Å] | 21.379(2) | 22.008(2) |
| α [deg] | 72.034(2) | 90.00 |
| β [deg] | 83.197(2) | 90.00 |
| γ [deg] | 67.743(3) | 90.00 |
| <i>V</i> [Å ³] | 6345.7(1) | 14662(2) |
| <i>Z</i> | 1 | 4 |
| ρ_{calcd} [g cm ⁻³] | 1.250 | 1.010 |
| μ [mm ⁻¹] | 0.641 | 0.539 |
| <i>F</i> (000) | 2352 | 4448 |
| $2\theta_{max}$ [deg] | 52.00 | 52.00 |
| no. of unique data | 24 805 | 14 421 |
| no. of param | 1299 | 618 |
| GOF [F^2] ^a | 1.02 | 1.07 |
| $R1$ [$F^2 > 2\sigma(F^2)$], $wR2$ [F^2] ^b | 0.0547, 0.1177 | 0.0535, 0.1325 |
| $\Delta\rho_{min}$ $\Delta\rho_{max}$ [e Å ⁻³] | −0.71, 0.99 | −0.33, 0.47 |

^aGOF = $[w(F_o^2 - F_c^2)^2]/(n - p)^{1/2}$, where *n* and *p* denote the number of data points and the number of parameters, respectively. ^b $R1 = (|F_o| - |F_c|)/|F_o|$; $wR2 = [w(F_o^2 - F_c^2)^2]/[w(F_o^2)^2]^{1/2}$, where $w = 1/[\sigma^2(F_o^2) + (aP)^2 + bP]$ and $P = (F_o^2 + 2F_c^2)/3$.

at room temperature under N_2 conditions. After the solution became clear, the solvent was removed and the resulting oil product was suspended in 30 mL of methanol under reflux. After 24 h, solvent was distilled; purification was achieved by column chromatography to afford pure product as a white or light-yellow powder.

General Pyrazole Preparation.²⁷ Hydrazine hydrate (2 mL, 80%) was added during a 10 min period to a stirred and refluxed solution of acetylacetone (8.4 mmol) in 20 mL of ethanol. After 12 h, the solvent was concentrated and filtered, and the resulting solid was washed twice with H_2O and vacuum-dried.

3,3'-(9-Methyl-9H-carbazole-3,6-diyl)bis(4-hydroxypent-3-en-2-one) (a). The above general acetylacetone preparation procedure was followed with 9-methylcarbazole-3,6-dicarbaldehyde (2.0 g, 8.4 mmol) to give **a** as a white powder. The product was vacuum-dried (634 mg, 20%). 1H NMR (400 MHz, $CDCl_3$, 25 °C, $Si(CH_3)_4$, ppm): δ 16.73 (s, 2H, −OH), 7.87 (s, 2H, Cz−H), 7.46–7.44 (d, *J* = 8.3 Hz, 2H, Cz−H), 7.31–7.28 (d, 2H, Cz−H), 3.93 (s, 3H, N−CH₃), 1.93 (s, 12H, −CH₃). ^{13}C NMR (100 MHz, $CDCl_3$, 25 °C, $Si(CH_3)_4$, ppm): δ

191.4, 140.6, 129.1, 127.8, 122.8, 115.5, 109.0, 29.3, 24.4. Elem anal. Calcd for $C_{23}H_{23}NO_4$: C, 73.19; H, 6.14; N, 3.71. Found: C, 73.17; H, 6.09; N, 3.69. ESI-MS anal. Calcd for $[C_{23}H_{23}NO_4 + Na]^+$: m/z 400.1519. Found: m/z 400.1521.

3,3'-(9-Benzyl-9H-carbazole-3,6-diyl)bis(4-hydroxypent-3-en-2-one) (b). The above general acetylacetone preparation procedure was followed with 9-benzylcarbazole-3,6-dicarbaldehyde (2.63 g, 8.4 mmol) to give **b** as a light-yellow powder. The product was vacuum-dried (762 mg, 20%). 1H NMR (400 MHz, $CDCl_3$, 25 °C, $Si(CH_3)_4$, ppm): δ 16.75 (s, 2H, -OH), 7.92–7.91 (d, J = 1.4 Hz, 2H, C $_z$ -H), 7.45–7.42 (d, J = 8.3 Hz, 2H, C $_z$ -H), 7.36–7.31 (m, 3H, Ar-H), 7.28–7.27 (d, J = 1.7, 2H, C $_z$ -H), 7.25 (m, 2H, Ar-H), 5.57 (s, 2H, -CH $_2$), 1.96 (s, 12H, -CH $_3$). ^{13}C NMR (100 MHz, $CDCl_3$, 25 °C, $Si(CH_3)_4$, ppm): δ 191.3, 140.8, 139.6, 138.4, 128.6, 128.1, 127.6, 126.4, 125.7, 118.3, 109.4, 46.9, 24.2. Elem anal. Calcd for $C_{29}H_{27}NO_4$: C, 76.80; H, 6.00; N, 3.09. Found: C, 76.82; H, 6.09; N, 3.03. ESI-MS anal. Calcd for $[C_{29}H_{27}NO_4 + Na]^+$: m/z : 476.1832. Found: m/z 476.1803.

3,3'-(9-Benzyl-9H-carbazole-3,6-diyl)bis(4,1-phenylene)]bis(4-hydroxypent-3-en-2-one) (c). The above general acetylacetone preparation procedure was followed with 4,4'-(9-benzylcarbazole-3,6-diyl)dibenzaldehyde (4.0 g, 8.4 mmol) to give **c** as a light-yellow powder. The product was vacuum-dried (1.02 g, 20%). 1H NMR (400 MHz, $CDCl_3$, 25 °C, $Si(CH_3)_4$, ppm): δ 16.74 (s, 2H, -OH), 8.47–8.45 (s, 2H, C $_z$ -H), 7.77–7.75 (d, J = 8.3 Hz, 4H, C $_z$ -Ar-H), 7.77–7.75 (covered, 2H, C $_z$ -H), 7.50–7.48 (d, J = 8.2 Hz, 2H, C $_z$ -H), 7.32–7.21 (m, 9H, C $_z$ -Ar-H and Ar-H), 5.61 (s, 2H, -CH $_2$), 1.99 (s, 12H, -CH $_3$). ^{13}C NMR (100 MHz, $CDCl_3$, 25 °C, $Si(CH_3)_4$, ppm): δ 191.1, 141.0, 140.8, 136.9, 135.1, 132.3, 131.6, 128.9, 127.7, 127.6, 126.5, 125.5, 123.8, 118.9, 114.9, 109.5, 46.9, 24.3. Elem anal. Calcd for $C_{41}H_{35}NO_4$: C, 81.30; H, 5.82; N, 2.31. Found: C, 81.27; H, 5.85; N, 2.32. ESI-MS anal. Calcd for $[C_{41}H_{35}NO_4 + Na]^+$: m/z 628.2488. Found: m/z 628.2403.

9-Methyl-3,6-bis[3-(trifluoromethyl)-1H-pyrazol-5-yl]-9H-carbazole (H_2L^1). The above general pyrazole preparation procedure was followed with 1,1'-(9-methylcarbazole-3,6-diyl)bis(4,4,4-trifluorobutane-1,3-dione) (755 mg, 1.68 mmol), and a white solid of H_2L^1 was obtained (717 mg, 95%). 1H NMR (400 MHz, DMSO- d_6 , 25 °C, $Si(CH_3)_4$, ppm): δ 14.06 (s, 2H, -NH), 8.66 (s, 2H, C $_z$ -H), 7.99–7.97 (d, J = 8.8 Hz, 2H, C $_z$ -H), 7.79–7.77 (d, J = 8.6 Hz, 2H, C $_z$ -H), 7.18 (s, 2H, -CH), 3.97 (s, 3H, N-CH $_3$).

3,6-Bis(3,5-dimethyl-1H-pyrazol-4-yl)-9-methyl-9H-carbazole (H_2L^2). The above general pyrazole preparation procedure was followed with **a** (634 mg, 1.68 mmol), and a white solid of H_2L^2 was obtained (590 mg, 95%). 1H NMR (400 MHz, DMSO- d_6 , 25 °C, $Si(CH_3)_4$, ppm): δ 12.23 (s, 2H, -NH), 8.08 (d, J = 1.3 Hz, 2H, C $_z$ -H), 7.62–7.60 (d, J = 8.3 Hz, 2H, C $_z$ -H), 7.38–7.35 (d, J_1 = 8.4 Hz, J_2 = 3.2 Hz, 2H, C $_z$ -H), 3.91 (s, 3H, N-CH $_3$), 2.23 (s, 12H, -CH $_3$). ^{13}C NMR (100 MHz, DMSO- d_6 , 25 °C, $Si(CH_3)_4$, ppm): δ 139.9, 127.6, 125.0, 122.8, 121.1, 118.4, 109.4, 56.5, 29.5, 19.0, 11.9. Elem anal. Calcd for $C_{23}H_{23}N_5 \cdot H_2O$: C, 71.29; H, 6.50; N, 18.07. Found: C, 71.37; H, 6.59; N, 18.01. ESI-MS anal. Calcd for $[C_{23}H_{23}N_5 + H]^+$: m/z 370.2026. Found: m/z 370.2037.

9-Benzyl-3,6-bis(3,5-dimethyl-1H-pyrazol-4-yl)-9H-carbazole (H_2L^3). The above general pyrazole preparation procedure was followed with **b** (762 mg, 1.68 mmol), and a white solid of H_2L^3 was obtained (711 mg, 95%). 1H NMR (400 MHz, DMSO- d_6 , 25 °C, $Si(CH_3)_4$, ppm): δ 12.23 (s, 2H, -NH), 8.11 (d, J = 1.2 Hz, 2H, C $_z$ -H), 7.66–7.63 (d, J = 8.5 Hz, 2H, C $_z$ -H), 7.24–7.35 (m, 7H, C $_z$ -H and Ar-H), 5.67 (s, 2H, N-CH $_2$), 2.09 (s, 12H, -CH $_3$). ^{13}C NMR (100 MHz, DMSO- d_6 , 25 °C, $Si(CH_3)_4$, ppm): δ 140.8, 139.4, 138.4, 129.1, 127.8, 127.6, 127.4, 125.3, 123.0, 121.2, 118.2, 109.8, 46.3, 11.9. Elem anal. Calcd for $C_{29}H_{27}N_5 \cdot 2H_2O$: C, 72.33; H, 6.49; N, 14.54. Found: C, 72.31; H, 6.49; N, 14.51. ESI-MS anal. Calcd for $[C_{29}H_{27}N_5 + H]^+$: m/z : 446.2339. Found: m/z 446.2315.

9-Benzyl-3,6-bis[4-(3,5-dimethyl-1H-pyrazol-4-yl)phenyl]-9H-carbazole (H_2L^4). The above general pyrazole preparation procedure was followed with **c** (1.02 g, 1.68 mmol), and a white solid of H_2L^4 was obtained (954 mg, 95%). 1H NMR (400 MHz, DMSO- d_6 , 25 °C, $Si(CH_3)_4$, ppm): δ 12.35 (s, 2H, -NH), 8.80 (d, J = 0.8 Hz, 2H, C $_z$ -

H), 7.86–7.80 (m, 6H, C $_z$ -H and C $_z$ -Ar-H), 7.75–7.73 (d, J = 8.5 Hz, 2H, C $_z$ -H), 7.43–7.40 (d, J = 8.2 Hz, 4H, Ar-H), 7.33–7.24 (m, 5H, Ar-H), 5.74 (s, 2H, -CH $_2$), 2.27 (s, 12H, -CH $_3$). ^{13}C NMR (100 MHz, DMSO- d_6 , 25 °C, $Si(CH_3)_4$, ppm): δ 141.0, 140.6, 138.9, 138.2, 132.6, 131.9, 129.6, 129.1, 127.8, 127.2, 125.4, 123.7, 119.2, 117.1, 110.5, 46.3, 12.0. Elem anal. Calcd for $C_{41}H_{35}N_5 \cdot H_2O$: C, 79.97; H, 6.06; N, 11.37. Found: C, 79.94; H, 6.08; N, 11.36. ESI-MS anal. Calcd for $[C_{41}H_{35}N_5 + H]^+$: m/z 598.2965. Found: m/z 598.2922. $[(phen)_8Pd_8L^1_4](NO_3)_8$ ($1 \cdot 8NO_3^-$), $[(phen)_8Pd_8L^1_4](PF_6)_8$ ($1 \cdot 8PF_6^-$), and $[(phen)_8Pd_8L^1_4](BF_4)_8$ ($1 \cdot 8BF_4^-$)

Self-Assembly of Metallomacrocycles General Procedures $[(phen)_2Pd_2(NO_3)_2](NO_3)_2$ (18.3 mg, 0.02 mmol) was added to a suspension of H_2L^1 (10 mg, 0.02 mmol) in a H_2O (1 mL) and acetone (0.5 mL) solution. The mixture was stirred for 2 h at room temperature and was then heated at 60 °C for another 24 h to react fully. After that, the resulting solution was filtered, and the clear yellow filtrate was evaporated to dryness to give a yellow solid of $1 \cdot 8NO_3^-$. Yield: 19 mg (67%). The PF_6^- salt of **1** ($1 \cdot 8PF_6^-$) was prepared by anion exchange of $1 \cdot 8NO_3^-$ with a 10-fold excess of KPF_6 in a methanol solution in quantitative yield. 1H NMR (400 MHz, CD_3CN , 25 °C, $Si(CH_3)_4$, ppm): δ 9.11 (s, 4H), 8.84–8.82 (d, J = 7.9 Hz, 4H), 8.79–8.77 (d, J = 8.0 Hz, 4H), 8.68–8.66 (d, J = 8.2 Hz, 4H), 8.65–8.64 (d, J = 5.4 Hz, 4H), 8.57–8.55 (d, J = 5.0 Hz, 4H), 8.40–8.38 (d, J = 8.2 Hz, 4H), 8.24–8.22 (d, J = 5.3 Hz, 4H), 8.15–8.12 (dd, J_1 = 8.3 Hz, J_2 = 1.5 Hz, 4H), 8.14 (s, 8H), 7.93–7.90 (d, J = 8.8 Hz, 4H), 7.91–7.88 (dd, J_1 = 8.2 Hz, J_2 = 5.5 Hz, 4H), 7.85–7.83 (d, J = 5.7 Hz, 4H), 7.83–7.81 (d, J = 7.9 Hz, 4H), 7.82–7.79 (d, J = 8.7 Hz, 4H), 7.76 (s, 4H), 7.76–7.72 (dd, J_1 = 8.2 Hz, J_2 = 5.5 Hz, 4H), 7.69–7.68 (d, J = 5.2 Hz, 4H), 7.63–7.61 (d, J = 8.5 Hz, 4H), 7.35–7.32 (dd, J_1 = 8.3 Hz, J_2 = 5.5 Hz, 4H), 7.25 (s, 4H), 6.95 (s, 4H), 6.67–6.65 (d, J = 8.5 Hz, 4H), 3.68 (s, 12H). ESI-MS (acetonitrile): m/z 1602.33 ($[1 \cdot 8PF_6^-]^{3+}$). Elem anal. Calcd for $C_{180}H_{108}N_{36}Pd_8P_8F_{72} \cdot 2H_2O$: C, 40.96; H, 2.14; N, 9.55. Found: C, 40.86; H, 2.34; N, 9.43. The BF_4^- salt of **1** ($1 \cdot 8BF_4^-$) was also obtained as yellow microcrystals in quantitative yield. X-ray-quality crystals were grown by the slow vapor diffusion of diethyl ether into a solution of $1 \cdot 8BF_4^-$ in acetonitrile at room temperature. $[(dmbpy)_4Pd_4L^1_2](NO_3)_4$ ($2 \cdot 4NO_3^-$) and $[(dmbpy)_4Pd_4L^1_2](BF_4)_4$ ($2 \cdot 4BF_4^-$)

The same procedure as that employed for $1 \cdot 8NO_3^-$ was used to make $2 \cdot 4NO_3^-$, except that $[(dmbpy)_2Pd_2(NO_3)_2](NO_3)_2$ (18.5 mg, 0.02 mmol) was used as the starting material. Yield: 21.4 mg (75%). The BF_4^- salt of **2** ($2 \cdot 4BF_4^-$) was prepared by anion exchange of $2 \cdot 4NO_3^-$ with a 10-fold excess of KBF_4 in a methanol solution in quantitative yield. 1H NMR (400 MHz, CD_3CN , 25 °C, $Si(CH_3)_4$, ppm): δ 8.92 (s, 2H), 8.25 (s, 2H), 8.20 (s, 2H), 8.15–8.14 (d, J = 5.9 Hz, 2H), 8.12–8.10 (d, J = 5.9 Hz, 2H), 8.03–8.00 (dd, J_1 = 8.5 Hz, J_2 = 1.7 Hz, 2H), 7.90 (s, 2H), 7.72 (s, 2H), 7.67 (s, 2H), 7.60–7.58 (d, J = 5.9 Hz, 2H), 7.57 (s, 2H), 7.54–7.52 (d, J = 8.5 Hz, 2H), 7.46–7.44 (d, J = 6.2 Hz, 2H), 7.35–7.33 (t, J = 4.7 Hz, 4H), 7.16–7.14 (d, J = 5.9 Hz, 2H), 6.90 (s, 2H), 6.84 (s, 2H), 6.82–6.80 (d, J = 8.6 Hz, 2H), 6.79–6.77 (d, J = 6.5 Hz, 2H), 3.76 (s, 6H), 2.59 (s, 8H), 2.56 (s, 8H), 2.42 (s, 8H). ESI-MS (acetonitrile): m/z 1115.61 ($[2 \cdot 2BF_4^-]^{2+}$) and 713.74 ($[2 \cdot 2BF_4^-]^{3+}$). Elem anal. Calcd for $C_{90}H_{70}N_{18}Pd_4B_4F_{28} \cdot H_2O$: C, 44.62; H, 3.00; N, 10.41. Found: C, 44.46; H, 2.84; N, 10.33. $[(phen)_4Pd_4L^2_2](NO_3)_4$ ($3 \cdot 4NO_3^-$) and $[(phen)_4Pd_4L^2_2](BF_4)_4$ ($3 \cdot 4BF_4^-$)

The same procedure as that employed for $1 \cdot 8NO_3^-$ was used to make $3 \cdot 4NO_3^-$, except that $[(phen)_2Pd_2(NO_3)_2](NO_3)_2$ (33.6 mg, 0.04 mmol) and H_2L^2 (15 mg, 0.04 mmol) were used as starting materials. Yield: 37.7 mg (80%). The BF_4^- salt of **3** ($3 \cdot 4BF_4^-$) was prepared by exchange with a 10-fold excess of KBF_4 in a methanol solution in quantitative yield. Pure $3 \cdot 4BF_4^-$, as a microcrystalline light-yellow solid, was obtained by the vapor diffusion of diethyl ether into a solution of $3 \cdot 4BF_4^-$ in acetonitrile at room temperature. Yield: 20 mg (53%). 1H NMR (400 MHz, CD_3CN , 25 °C, $Si(CH_3)_4$, ppm): δ 9.08–9.06 (d, J = 8.2 Hz, 8H, phen-H), 8.70–8.69 (d, J = 4.9 Hz, 8H, phen-H), 8.35 (s, 8H, phen-H), 8.19–8.15 (dd, J_1 = 8.2 and 5.3 Hz, 8H, phen-H), 8.15 (s, 4H, C $_z$ -H), 7.75–7.73 (d, J = 8.7 Hz, 4H, C $_z$ -H), 7.68–7.65 (d, J = 8.6 Hz, 4H, C $_z$ -H), 3.98 (s, 6H, N-CH $_3$), 2.60 (s, 24H, L 2 -CH $_3$). ESI-MS (acetonitrile): m/z 1027.63 ($[3 \cdot 2BF_4^-]^{2+}$).

Elem anal. Calcd for $C_{94}H_{74}N_{18}Pd_4B_4F_{16}H_2O$: C, 50.25; H, 3.41; N, 11.22. Found: C, 50.09; H, 3.34; N, 11.06. X-ray-quality crystals were grown by the slow vapor diffusion of diethyl ether into a solution of $3\text{-}4BF_4^-$ in acetonitrile at room temperature. $[(dmbpy)_4Pd_4L^2_2](NO_3)_4$ ($4\text{-}4NO_3^-$) and $[(dmbpy)_4Pd_4L^2_2](BF_4)_4$ ($4\text{-}4BF_4^-$)

The same procedure as that employed for $1\text{-}8NO_3^-$ was used to make $4\text{-}4NO_3^-$, except that $[(dmbpy)_2Pd_2(NO_3)_2](NO_3)_2$ (33.8 mg, 0.04 mmol) and H_2L^2 (15 mg, 0.04 mmol) were used as starting materials. Yield: 37.7 mg (80%). 1H NMR (400 MHz, CD_3OD , 25 °C, $Si(CH_3)_4$, ppm): δ 8.46 (s, 8H, dmbpy-H), 8.21–8.19 (d, J = 5.8 Hz, 8H, dmbpy-H), 8.15 (s, 4H, Cz-H), 7.63–7.62 (d, J = 5.6 Hz, 8H, dmbpy-H), 7.62–7.60 (d, J = 8.5 Hz, 4H, Cz-H), 7.56–7.54 (dd, J_1 = 8.4 Hz, J_2 = 1.3 Hz, 4H, Cz-H), 3.96 (s, 6H, N-CH₃), 2.64 (s, 24H, L^2 -CH₃), 2.56 (s, 24H, dmbpy-CH₃). Elem anal. Calcd for $C_{94}H_{90}N_{22}Pd_4O_{12}H_2O$: C, 52.18; H, 4.29; N, 14.24. Found: C, 52.09; H, 4.34; N, 14.06.

The BF_4^- salt of **4** ($4\text{-}4BF_4^-$) was obtained as yellow microcrystals in quantitative yield after anion exchange. 1H NMR (400 MHz, CD_3CN , 25 °C, $Si(CH_3)_4$, ppm): δ 8.26 (s, 8H, dmbpy-H), 8.14–8.13 (d, J = 1.0 Hz, 4H, Cz-H), 8.12–8.10 (d, J = 5.7 Hz, 8H, dmbpy-H), 7.67–7.64 (d, J = 8.5 Hz, 4H, Cz-H), 7.60–7.58 (dd, J_1 = 8.4 Hz, J_2 = 1.6 Hz, 4H, Cz-H), 7.53–7.52 (d, J = 5.1 Hz, 8H, dmbpy-H), 3.96 (s, 6H, N-CH₃), 2.60 (s, 24H, L^2 -CH₃), 2.55 (s, 24H, dmbpy-CH₃). ESI-MS (acetonitrile): m/z 661.45 ($[4\text{-}BF_4^-]^{3+}$) and 474.39 ($[4]^{4+}$). Elem anal. Calcd for $C_{94}H_{90}N_{18}Pt_4B_4F_{16}H_2O$: C, 49.90; H, 4.10; N, 11.14. Found: C, 49.76; H, 4.13; N, 11.23. $[(phen)_4Pd_4L^3_2](NO_3)_4$ ($5\text{-}4NO_3^-$) and $[(phen)_4Pd_4L^3_2](BF_4)_4$ ($5\text{-}4BF_4^-$)

The same procedure as that employed for $1\text{-}8NO_3^-$ was used to make $5\text{-}4NO_3^-$, except that H_2L^3 (10 mg, 0.02 mmol) was used as the starting material. Yield: 21.5 mg (85%). 1H NMR (400 MHz, CD_3OD , 25 °C, $Si(CH_3)_4$, ppm): δ 9.02–9.00 (d, J = 8.2 Hz, 8H, phen-H), 8.80–8.79 (d, J = 5.0 Hz, 8H, phen-H), 8.33 (s, 4H, Cz-H), 8.30 (s, 8H, phen-H), 8.15–8.12 (dd, J_1 = 8.2 Hz, J_2 = 5.3 Hz, 8H, phen-H), 7.76–7.74 (d, J = 8.4 Hz, 4H, Cz-H), 7.71–7.69 (d, J = 8.4 Hz, 4H, Cz-H), 7.41–7.33 (m, 10H, Ar-H), 5.77 (s, 4H, Ar-CH₂), 2.73 (s, 24H, L^3 -CH₃). Elem anal. Calcd for $C_{106}H_{82}N_{22}O_{12}Pd_4\cdot 2H_2O$: C, 54.93; H, 3.74; N, 13.30. Found: C, 54.75; H, 3.81; N, 13.25.

The BF_4^- salt of **5** ($5\text{-}4BF_4^-$) was obtained as yellow microcrystals in quantitative yield after anion exchange. 1H NMR (400 MHz, CD_3CN , 25 °C, $Si(CH_3)_4$, ppm): δ 8.88–8.85 (dd, J_1 = 8.3 Hz, J_2 = 1.0 Hz, 8H, phen-H), 8.65–8.64 (dd, J_1 = 5.3 Hz, J_2 = 1.0 Hz, 8H, phen-H), 8.26 (d, J = 1.2 Hz, 4H, Cz-H), 8.20 (s, 8H, phen-H), 8.02–7.99 (dd, J_1 = 8.3 Hz, J_2 = 5.3 Hz, 8H, phen-H), 7.74–7.72 (d, J = 8.4 Hz, 4H, Cz-H), 7.68–7.65 (dd, J_1 = 8.4 Hz, J_2 = 1.5 Hz, 4H, Cz-H), 7.40–7.31 (m, 10H, Ar-H), 5.73 (s, 4H, Ar-CH₂), 2.68 (s, 24H, L^3 -CH₃). ESI-MS (acetonitrile): m/z 1103.67 ($[5\text{-}2BF_4^-]^{2+}$), 706.44 ($[5\text{-}BF_4^-]^{3+}$), and 508.33 ($[5]^{4+}$). Elem anal. Calcd for $C_{106}H_{82}N_{18}Pd_4B_4F_{16}\cdot 2H_2O$: C, 52.68; H, 3.59; N, 10.43. Found: C, 52.65; H, 3.61; N, 10.55. $[(dmbpy)_4Pd_4L^3_2](NO_3)_4$ ($6\text{-}4NO_3^-$) and $[(dmbpy)_4Pd_4L^3_2](BF_4)_4$ ($6\text{-}4BF_4^-$)

The same procedure as that employed for $1\text{-}8NO_3^-$ was used, except that H_2L^3 (10 mg, 0.02 mmol) and $[(dmbpy)_2Pd_2(NO_3)_2](NO_3)_2$ (18.4 mg, 0.02 mmol) were used as starting materials to give a yellow solid $6\text{-}4NO_3^-$. Yield: 24.7 mg (87%). 1H NMR (400 MHz, CD_3OD , 25 °C, $Si(CH_3)_4$, ppm): δ 8.46 (s, 8H, dmbpy-H), 8.19 (s, 8H, dmbpy-H), 8.18 (s, 4H, Cz-H), 7.62–7.60 (d, J = 5.7 Hz, 8H, dmbpy-H), 7.60–7.58 (d, J = 8.8 Hz, 4H, Cz-H), 7.52–7.50 (dd, J_1 = 8.4 Hz, J_2 = 1.6 Hz, 4H, Cz-H), 7.33–7.24 (m, 10H, Ar-H), 5.68 (s, 4H, Ar-CH₂), 2.63 (s, 24H, L^3 -CH₃), 2.56 (s, 24H, dmbpy-CH₃). Elem anal. Calcd for $C_{106}H_{98}N_{22}O_{12}Pd_4\cdot 2H_2O$: C, 54.55; H, 4.41; N, 13.20. Found: C, 54.75; H, 4.27; N, 13.15.

The BF_4^- salt of **6** ($6\text{-}4BF_4^-$) was obtained as yellow microcrystals in quantitative yield after anion exchange. 1H NMR (400 MHz, CD_3CN , 25 °C, $Si(CH_3)_4$, ppm): δ 8.25 (s, 8H, dmbpy-H), 8.16 (d, J = 1.2 Hz, 4H, Cz-H), 8.10–8.08 (d, J = 5.8 Hz, 8H, dmbpy-H), 7.68–7.66 (d, J = 8.5 Hz, 4H, Cz-H), 7.56–7.54 (dd, J_1 = 8.4 Hz, J_2 = 1.6 Hz, 4H, Cz-H), 7.51–7.50 (d, J = 5.5 Hz, 8H, dmbpy-H), 7.34–7.27 (m, 10H, Ar-H), 5.68 (s, 4H, Ar-CH₂), 2.60 (s, 24H, L^3 -CH₃), 2.54 (s, 24H, dmbpy-CH₃). ESI-MS (acetonitrile): m/z 1111.67 ($[6\text{-}2BF_4^-]^{2+}$), 712.18 ($[6\text{-}BF_4^-]^{3+}$), and 512.43 ($[6]^{4+}$). Elem anal.

Calcd for $C_{106}H_{98}N_{18}Pd_4B_4F_{16}\cdot 2H_2O$: C, 52.33; H, 4.23; N, 10.36. Found: C, 52.25; H, 4.52; N, 10.27. $[(15\text{-crown-5-phen})_4Pd_4L^4_2](NO_3)_4$ ($7\text{-}4NO_3^-$) and $[(15\text{-crown-5-phen})_4Pd_4L^4_2](PF_6)_4$ ($7\text{-}4PF_6^-$) The same procedure as that employed for $1\text{-}8NO_3^-$ was used, except that H_2L^4 (10 mg, 0.02 mmol) and $[(15\text{-crown-5-phen})_2Pd_2(NO_3)_2](NO_3)_2$ (20.0 mg, 0.02 mmol) were used as starting materials to give a yellow solid of $7\text{-}4NO_3^-$. Yield: 22.5 mg (75%). The PF_6^- salt of **7** ($7\text{-}4PF_6^-$) was obtained as yellow microcrystals in quantitative yield. 1H NMR (400 MHz, CD_3CN , 25 °C, $Si(CH_3)_4$, ppm): δ 8.98–8.96 (d, J = 8.6 Hz, 8H, phen-H), 8.62 (s, 4H, Cz-H), 8.49–8.48 (d, J = 5.3 Hz, 8H, phen-H), 7.98–7.95 (d, J = 8.4 Hz, 8H, phen-H), 7.96–7.94 (d, J = 8.3 Hz, 8H, Cz-Ar-H), 7.91–7.89 (dd, J_1 = 8.7 Hz, J_2 = 1.4 Hz, 4H, Cz-H), 7.71–7.69 (d, J = 8.4 Hz, 4H, Cz-H), 7.65–7.63 (d, J = 8.2 Hz, 8H, Cz-Ar-H), 7.39–7.27 (m, 10H, Ar-H), 5.74 (s, 4H, Ar-CH₂), 3.73–3.66 (m, 64H, crown-H), 2.65 (s, 24H, L^4 -CH₃). ESI-MS (acetonitrile): m/z 1080.91 ($[7\text{-}PF_6^-]^{3+}$) and 774.69 ($[7]^{4+}$). Elem anal. Calcd for $C_{162}H_{154}F_{24}P_4N_{18}Pd_4O_{20}\cdot 3H_2O$: C, 52.13; H, 4.32; N, 6.75. Found: C, 52.06; H, 4.37; N, 6.84. $[(dmbpy)_4Pd_4L^4_2](NO_3)_4$ ($8\text{-}4NO_3^-$) and $[(dmbpy)_4Pd_4L^4_2](BF_4)_4$ ($8\text{-}4BF_4^-$)

The same procedure as that employed for $1\text{-}8NO_3^-$ was used, except that H_2L^4 (10 mg, 0.02 mmol) and $[(dmbpy)_2Pd_2(NO_3)_2](NO_3)_2$ (13.9 mg, 0.02 mmol) were used as starting materials to give a yellow solid $8\text{-}4NO_3^-$. Yield: 13.2 mg (55%). The BF_4^- salt of **8** ($8\text{-}4BF_4^-$) was obtained as yellow microcrystals in quantitative yield. 1H NMR (400 MHz, CD_3CN , 25 °C, $Si(CH_3)_4$, ppm): δ 8.59 (d, J = 1.4 Hz, 4H, Cz-H), 8.23 (s, 8H, dmbpy-H), 8.01–8.00 (d, J = 5.9 Hz, 8H, dmbpy-H), 7.91–7.89 (d, J = 8.2 Hz, 8H, Cz-Ar-H), 7.86–7.84 (dd, J_1 = 8.6 Hz, J_2 = 1.6 Hz, 4H, Cz-H), 7.67–7.65 (d, J = 8.5 Hz, 4H, Cz-H), 7.56–7.54 (d, J = 8.2 Hz, 8H, Cz-Ar-H), 7.50–7.49 (d, J = 5.2 Hz, 8H, dmbpy-H), 7.36–7.24 (m, 10H, Ar-H), 5.71 (s, 4H, Ar-CH₂), 2.59 (s, 24H, L^4 -CH₃), 2.51 (s, 24H, dmbpy-CH₃). ESI-MS (methanol): m/z 587.64 ($[8]^{4+}$). Elem anal. Calcd for $C_{130}H_{114}F_{16}B_4N_{18}Pd_4\cdot 3H_2O$: C, 56.67; H, 4.39; N, 9.15. Found: C, 56.76; H, 4.47; N, 9.24.

■ ASSOCIATED CONTENT

Supporting Information

1H and ^{13}C NMR spectra of H_2L^1 , H_2L^2 , H_2L^3 , and H_2L^4 , 1H NMR spectra of **2–8** and ESI-MS spectra of **1–4** and **6–8**, UV–vis and fluorescence spectra, 1H NMR spectrum of $1\text{-}8PF_6^-$ interacted with SCN^- , crystal packings of complexes $1\text{-}8BF_4^-$ and $3\text{-}4BF_4^-$, tables of selected bond lengths and angles for $1\text{-}8BF_4^-$ and $3\text{-}4BF_4^-$, and X-ray crystallographic files for complexes $1\text{-}8BF_4^-$ and $3\text{-}4BF_4^-$ in CIF format. This material is available free of charge via the Internet at <http://pubs.acs.org>.

■ AUTHOR INFORMATION

Corresponding Author

*E-mail: yusy@ruc.edu.cn.

Notes

The authors declare no competing financial interest.

■ ACKNOWLEDGMENTS

This project was supported by the Fundamental Research Funds for the Central Universities and the Research Funds of Renmin University of China (Grant 11XNL011), the National Natural Science Foundation of China (Grants 51073171 and 91127039), and the Beijing Natural Science Foundation (Grant 2112018).

■ REFERENCES

- (a) Lehn, J.-M. *Supramolecular Chemistry, Concepts and Perspectives*; VCH: Weinheim, Germany, 1995. (b) Lehn, J.-M. *Templating, Self-Assembly, and Self-Organization*. In *Comprehensive*

Supramolecular Chemistry; Sauvage, J.-P., Hosseini, M. W., Eds.; Pergamon: New York, 1996.

- (2) (a) Fujita, M.; Ogura, K. *Coord. Chem. Rev.* **1996**, *148*, 249. (b) Fujita, M. *Chem. Soc. Rev.* **1998**, *27*, 417. (c) Fujita, M.; Tominaga, M.; Hori, A.; Therrien, B. *Acc. Chem. Res.* **2005**, *38*, 369.
- (3) (a) Stang, P. J.; Leininger, S.; Olenyuk, B. *Chem. Rev.* **2000**, *100*, 853. (b) Seidel, S. R.; Stang, P. J. *Acc. Chem. Res.* **2002**, *35*, 972–983. (c) Northrop, B. H.; Zheng, Y.-R.; Chi, K.-W.; Stang, P. J. *Acc. Chem. Res.* **2009**, *42*, 1554–1563.
- (4) (a) Saalfrank, R. W.; Maid, H.; Scheurer, A. *Angew. Chem., Int. Ed.* **2008**, *47*, 8794–8824. (b) Cotton, F. A.; Lin, C.; Murillo, C. A. *Acc. Chem. Res.* **2001**, *34*, 759. (c) Holliday, B. J.; Mirkin, C. A. *Angew. Chem., Int. Ed.* **2001**, *40*, 2022–2043. (d) Raymond, K. N.; Caulder, D. L. *Acc. Chem. Res.* **1999**, *32*, 975. (e) Yu, S.-Y.; Li, S.-H.; Huang, H.-P.; Zhang, Z.-X.; Jiao, Q.; Shen, H.; Hu, X.-X.; Huang, H. *Curr. Org. Chem.* **2005**, *9*, 555–563.
- (5) (a) Fujita, M.; Sun, Q.-F.; Iwasa, J.; Ogawa, D.; Ishido, Y.; Sato, S.; Ozeki, T.; Sei, Y.; Yamaguchi, K. *Science* **2010**, *328*, 1144. (b) Horiuchi, S.; Murase, T.; Fujita, M. *J. Am. Chem. Soc.* **2011**, *133*, 12445. (c) Fujita, M.; Li, D.; Zhou, W.; Landskron, K.; Sato, S.; Kiely, C. J.; Liu, T.-B. *Angew. Chem., Int. Ed.* **2011**, *50*, 5182. (d) Yoshizawa, M.; Klosterman, J. K.; Fujita, M. *Angew. Chem., Int. Ed.* **2009**, *48*, 3418–3438. (e) Schneider, H. J.; Yatsimirsky, A. K. *Chem. Soc. Rev.* **2008**, *37*, 263.
- (6) Kalck, P.; Dessoudeix, M. *Coord. Chem. Rev.* **1999**, *192*, 1185.
- (7) (a) Yu, S.-Y.; Zhang, Z.-X.; Cheng, E. C.-C.; Li, Y.-Z.; Yam, V. W.-W.; Huang, H.-P.; Zhang, R. J. *Am. Chem. Soc.* **2005**, *127*, 17944–17995. (b) Yu, S.-Y.; Sun, Q.-F.; Lee, T. K.-M.; Cheng, E. C.-C.; Li, Y.-Z.; Yam, V. W.-W. *Angew. Chem., Int. Ed.* **2008**, *47*, 4551–4554. (c) Sun, Q.-F.; Lee, T. K.-M.; Li, P.-Z.; Yao, L.-Y.; Huang, J.-J.; Huang, J.; Yu, S.-Y.; Li, Y.-Z.; Cheng, E. C.-C.; Yam, V. W.-W. *Chem. Commun.* **2008**, *43*, 5514–5516.
- (8) (a) Yam, V. W.-W.; Cheng, E. C.-C. *Chem. Soc. Rev.* **2008**, *37*, 1806. (b) Yam, V. W.-W.; Wong, K. M.-C. *Acc. Chem. Res.* **2011**, *44*, 424.
- (9) (a) Beer, P. D.; Gale, P. A. *Angew. Chem., Int. Ed.* **2001**, *40*, 486. (b) Beer, P. D.; Hayes, E. J. *Coord. Chem. Rev.* **2003**, *240*, 167. (c) Gale, P. A.; Fisher, M. G.; Light, M. E.; Loeb, S. J. *Chem. Commun.* **2008**, 5695. (d) Gale, P. A. *Chem. Commun.* **2011**, *47*, 82. (e) Martinez-Manez, R.; Sancenon, F. *Coord. Chem. Rev.* **2006**, *250*, 3081. (f) Loeb, S. J.; Mercer, D. J. *Chem. Soc. Rev.* **2010**, *39*, 3612. (g) Kubik, S. *Chem. Soc. Rev.* **2010**, *39*, 3648–3663.
- (10) (a) Bondy, C. R.; Gale, P. A.; Loeb, S. J. *J. Am. Chem. Soc.* **2004**, *126*, 5030–5031. (b) Vega, I. E. D.; Gale, P. A.; Light, M. E.; Loeb, S. J. *Chem. Commun.* **2005**, 4913–4915.
- (11) (a) Yu, S.-Y.; Huang, H.; Liu, H.-B.; Chen, Z.-N.; Zhang, R.; Fujita, M. *Angew. Chem., Int. Ed.* **2003**, *42*, 686–690. (b) Li, S.-H.; Huang, H.-P.; Yu, S.-Y.; Li, Y.-Z.; Huang, H.; Sei, Y.; Yamaguchi, K. *Dalton Trans.* **2005**, 2346–2348. (c) Li, X.; Li, H.; Yu, S.-Y.; Li, Y.-Z. *Sci. China, Ser. B: Chem.* **2009**, *52*, 471–474. (d) Yao, L.-Y.; Qin, L.; Xie, T.-Z.; Li, Y.-Z.; Yu, S.-Y. *Inorg. Chem.* **2011**, *50*, 6055–6062.
- (12) (a) Yu, S.-Y.; Huang, H.-P.; Li, S.-H.; Jiao, Q.; Li, Y.-Z.; Wu, B.; Sei, Y.; Yamaguchi, K.; Pan, Y.-J.; Ma, H.-W. *Inorg. Chem.* **2005**, *44*, 9471–9488. (b) Yu, S.-Y.; Jiao, Q.; Li, S.-H.; Huang, H.-P.; Li, Y.-Z.; Pan, Y.-J.; Yamaguchi, K. *Org. Lett.* **2007**, *9*, 1379–1382. (c) Sun, Q.-F.; Liu, L.-X.; Huang, H.-P.; Yu, S.-Y.; Yam, V. W.-W. *Inorg. Chem.* **2008**, *47*, 2142–2145. (d) Ning, G.-H.; Yao, L.-Y.; Liu, L.-X.; Xie, T.-Z.; Li, Y.-Z.; Qin, Y.; Pan, Y.-J.; Yu, S.-Y. *Inorg. Chem.* **2010**, *49*, 7783–7792.
- (13) (a) Deacon, G. B.; Forsyth, C. M.; Gitlits, A.; Harika, R.; Junk, P. C.; Skelton, B. W.; White, A. H. *Angew. Chem., Int. Ed.* **2002**, *41*, 3249–3251. (b) Kozimor, S. A.; Bartlett, B. M.; Rinehart, J. D.; Long, J. R. *J. Am. Chem. Soc.* **2007**, *129*, 10672–10674. (c) Dias, H. V. R.; Diyabalanage, H. V. K.; Eldabaja, M. G.; Elbjeirami, O.; Rawashdeh-Omary, M. A.; Franzman, M. A.; Omary, M. A. *J. Am. Chem. Soc.* **2005**, *127*, 7489–7501. (d) Dias, H. V. R.; Singh, S.; Campana, C. F. *Inorg. Chem.* **2008**, *47*, 3943. (e) Salles, F.; Maurin, G.; Serre, C.; Llewellyn, P. L.; Knöfel, C.; Choi, H. J.; Filinchuk, Y.; Oliviero, L.; Vimont, A.; Long, J. R.; Férey, G. *J. Am. Chem. Soc.* **2010**, *132*, 13782–13788.
- (f) Deacon, G. B.; Delbridge, E. E.; Forsyth, C. M. *Angew. Chem., Int. Ed.* **1999**, *38*, 1766–1767. (g) He, J.; Yin, Y.-G.; Wu, T.; Li, D.; Huang, X.-C. *Chem. Commun.* **2006**, 2845–2847.
- (14) (a) Trofimenko, S. *Chem. Rev.* **1972**, *72*, 497–509. (b) Trofimenko, S. *Prog. Inorg. Chem.* **1986**, *34*, 115–210. (c) Sadimenko, A. P.; Bassoon, S. S. *Coord. Chem. Rev.* **1996**, *147*, 247–297. (d) La Monica, G.; Ardizzoia, G. A. *Prog. Inorg. Chem.* **1997**, *46*, 151–238. (e) Vela, J.; Vaddadi, S.; Kingsley, S.; Flaschenriem, C. J.; Lachicotte, R. J.; Cundari, T. R.; Holland, P. L. *Angew. Chem., Int. Ed.* **2006**, *45*, 1607–1611.
- (15) Yu, S.-Y.; Fujita, M.; Yamaguchi, K. *J. Chem. Soc., Dalton Trans.* **2001**, 3415.
- (16) Huang, H.-P.; Li, S.-H.; Yu, S.-Y.; Li, Y.-Z.; Jiao, Q.; Pan, Y.-J. *Inorg. Chem. Commun.* **2005**, *8*, 656–660.
- (17) (a) Gale, P. A. *Coord. Chem. Rev.* **2000**, *199*, 181–233. (b) Gale, P. A. *Coord. Chem. Rev.* **2001**, *213*, 79–128.
- (18) CAChe6.1.1 for Windows; Fujitsu Ltd.: Chiba, Japan, 2003.
- (19) Armarego, W. L. F.; Perrin, D. D. *Purification of Laboratory Chemicals*, 4th ed.; Butterworth Heinemann: Oxford, U.K., 1997.
- (20) Conrad, R. C.; Rund, J. V. *Inorg. Chem.* **1972**, *11*, 129–134.
- (21) Rice, C. R.; Guerrero, A.; Bell, Z. R.; Paul, R. L.; Motson, G. R.; Jeffery, J. C.; Ward, M. D. *New J. Chem.* **2001**, *25*, 185.
- (22) Zhang, Y.-D.; Zhang, L.-M.; Hiroyuki, S. *Macromolecules* **1996**, *29*, 1569–1573.
- (23) (a) Teki, Y.; Miyamoto, S.; Nakatsuji, M.; Miura, Y. *J. Am. Chem. Soc.* **2001**, *123*, 294–305. (b) Zhang, W.; Moore, J. S. *J. Am. Chem. Soc.* **2004**, *126*, 12796.
- (24) Cheng, L.-P.; Li, L.; Sun, P.-P.; Zhou, H.-P.; Tian, Y.-P.; Tang, H.-H. *Sci. China, Ser. B: Chem* **2009**, *52*, 529–534.
- (25) Sheldrick, G. M. *SADABS, Program for area detector adsorption correction*; Institute for Inorganic Chemistry, University of Göttingen, Göttingen, Germany, 1996.
- (26) Sheldrick, G. M. *SHELXTL, Program for Solution and Refinement of Crystal Structures*, version 5.1; University of Göttingen: Göttingen, Germany, 1997.
- (27) (a) Ramirez, F.; Bhatia, S. B.; Patwardhan, A. V.; Smith, C. P. *J. Org. Chem.* **1967**, *32*, 2194–2199. (b) Ramirez, F.; Bhatia, S. B.; Patwardhan, A. V.; Smith, C. P. *J. Org. Chem.* **1967**, *32*, 3547–3553.